Geological overwiew of Gandharan sites and petrographical analysis on Gandharan stucco and clay artefacts

Carlo Rosa
Sigea Lazio, Istituto Italiano di Paleontologia Umana
Thomas Theye
University of Stuttgart
Simona Pannuzi
MIBAC, Istituto Superiore per la Conservazione ed il Restauro

opposite page

Sample BKG 1123 15C: architectonical polycrome decoration from Barikot, Pakistan: the arrow indicates the traces of red colour (photo E. Loliva © ISCR).

Abstract

The Gandharan archaeological sites are mostly located in the Indus Suture Zone and in the lower Swat. In a recent past, scholars observed the use of local different type of schists to build buildings and sacred artworks. In this new research we highlighted the use of limestone for stucco artefacts and architectural decorations. This limestone is not a local rock in Swat but its main, extended and closer outcrops are located in the mountains northwest of Islamabad. Indeed, through specific analyses carried out by our team, the compatibility of these outcrops with the rocks used for stucco artefacts and stucco decorations of buildings was observed. This stucco was made by a mixture of different kinds of local crushed rocks (i.e. schists and granites).

Keywords
Limestone, clay artefacts, stucco decorations, Gandharan artefacts, Swat geology, petrographic analysis.

Geological introduction

The formation of the Himalaya mountain range is due to the collision between Eurasia and the north-western side of the Indian Plate, moving from the south, since the Mesozoic Era and up to the present days[1]. The northern termination of the Indian Plate is defined by the Indus-Tsangpo suture zone[2]. This suture zone continues westwards to the Swat area of Pakistan, where it is called "Main Mantle Thrust" – henceforth MMT [3] –. The MMT separates the metamorphic Kohistan island arc sequence north, from the metamorphic continental basement of the Indian plate in the south. The Suture Zone itself consists of a mélange of klippen of various rock types (Fig.1). The Swat valley is located between the Indian Plate and the Kohistan island arc sequences and the Swat River flows in part inside the tectonic lineament called MMT, a zone intensively fractured and erodible[4].
In northern Pakistan the geological succession from south to the north is formed by the following rock formations (Fig. 3):

1. Indian plate continental crust – lower Swat

The lower Swat sequence occurring in the lowermost tectonic position (Manglaur Formation) consists of a high-grade metamorphic augen

[1] Yin, Harrison 2000; Ding et al. 2005: the scholars dated the start of collision to Cenozoic (65-60 My).

[2] Gansser 1980.

[3] Jan, Tahirkheli 1969; Tahirkheli 1979a and 1979b; Tahirkheli 1980.

[4] Faccenna et al. 1993, pp.257-161.

RA 2 | 2019, pagg. 10 | 35
ISSN 1724-9686 (print) | ISSN 2465-2377 (online)

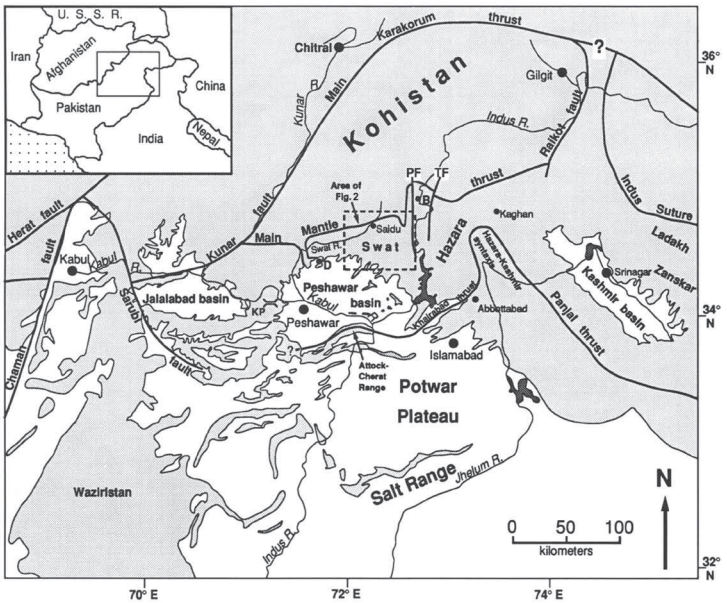

Fig. 1
Map of Northern Pakistan: shaded area represents pre-Quaternary rock (from Dipietro et al. 1991, fig.1).

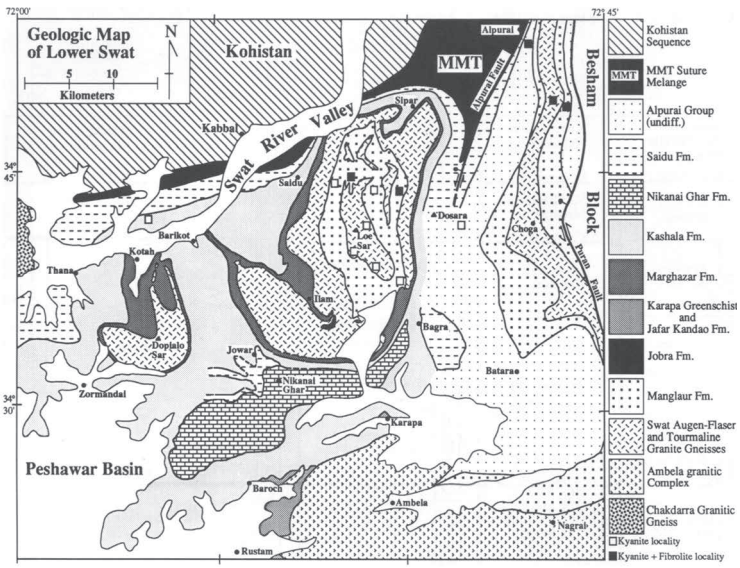

Fig. 2
Geological map of Lower Pakistan (from Dipietro et al. 1991, fig.3).

gneiss, of a tourmaline-bearing granite gneiss and associated metasediments. The metasediments include garnet-bearing micaschists, with parts of kyanite, quartzite, amphibolites, and tremolite marble[5]. This lower Swat sequence is overlaied by subcontinental, low to intermediate grade metamorphic rocks (Alpurai group, Saidu schists). Major rock types in the Alpurai groups are amphibolite schists, mica schists (partly with garnet), calcareous schists, graphitic phyllites, and calc-silicate marbles. Undeformed tourmaline-bearing granite is also attested (Fig. 2).

[5] Dipietro, Lawrence 1991.

2. Indus Suture Zone – separating 1 and 3 zones

The rock types in the suture zone itself includes blocks of low-grade metavolcanics, ultramafic rocks, sheared greenschists, serpentinite, talc-dolomite schists and blueschists[6]. For detailed description of all rock formations and their stratigraphical relationships, the paper of Kazmi et al. in 1984 was a milestone in the geological research of this area[7]. Noteworthy is the occurrence of emerald, close to Mingora[8]. Considered as a whole, the rock assemblage represents a typical, metamorphosed and sheared, ophiolitic mélange association found at convergent plate boundaries (Fig.1).

3. Kohistan island arc association in the north

Major rock types in this unit are calc-alkaline volcanics and intrusives rocks of various metamorphic grade (greenschists, amphibolites, granulites, non-metamorphic) and metasediments (Fig. 3).

Alluvial deposits cover the basement in the Swat river valley. Because of the NE-SW trend of the valley, it is expected that the deposits are fed both from the north and the south. It is important to note the complete absence of limestone outcrops in the Swat valley and surrounding areas (Fig. 3), where the main Gandharan sites are located. In these sites the presence of structures built with limestone and stucco is widespread. The nearest limestone outcrops are located in the north-western area of Islamabad (Fig. 4)[9].

Indeed, a geological overview of the Gandharan settlement in Afghanistan, in northern and southern areas of Kabul, shows the presence of different

Fig. 3
Geological map of Pakistan by Geological Survey of Pakistan and U.S. Geological Survey 1964 (detail).

[6] Tahirkheli et al., 1979a; Kazmi et al., 1984.

[7] Kazmi et al., 1984.

[8] Kazmi et al., 1986.

[9] Williams et al., 1988-90.

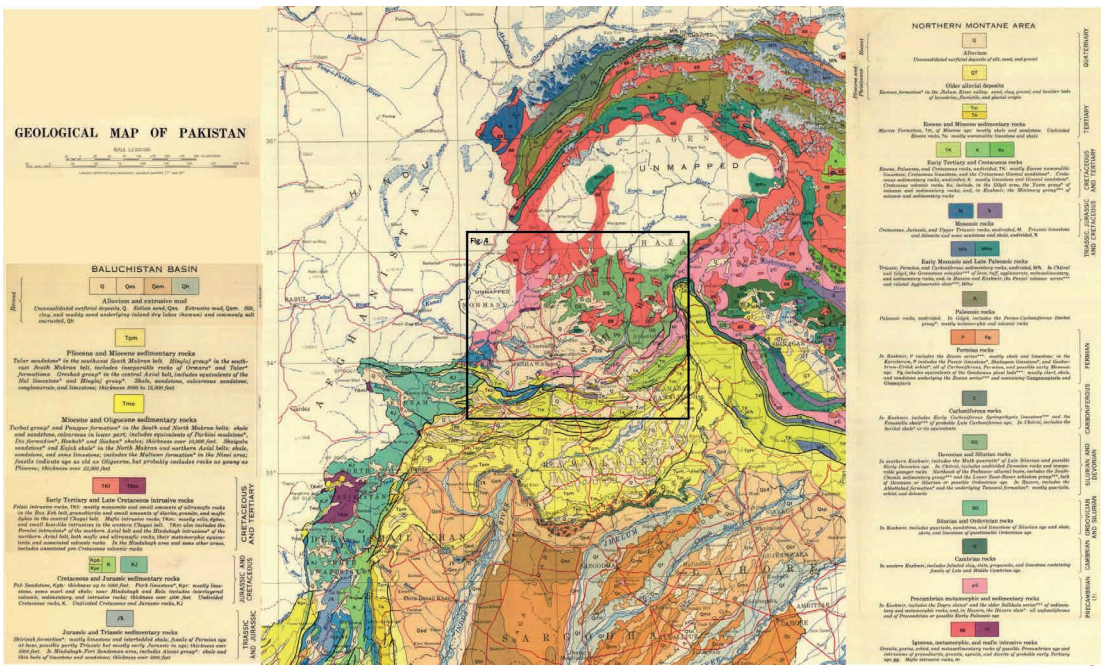

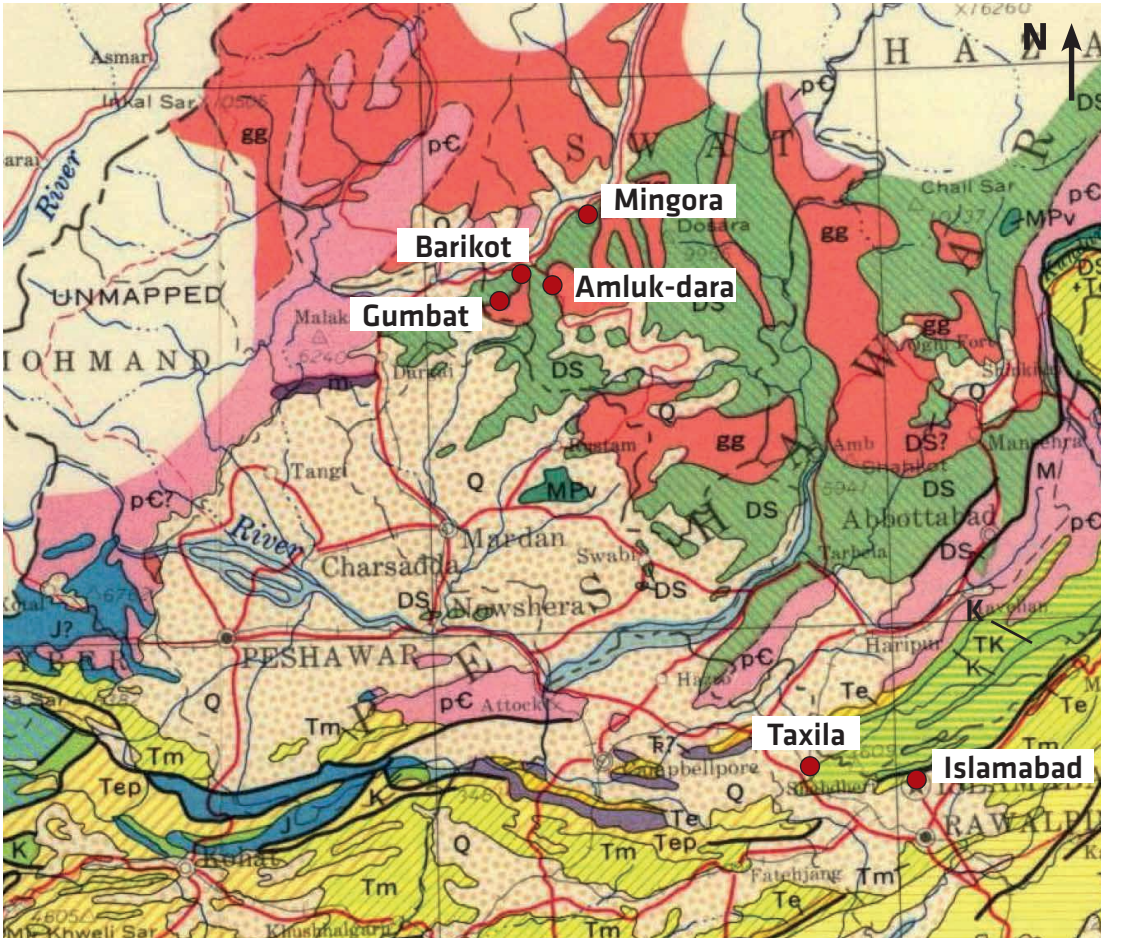

Fig. 4
Islamabad area in Geological Map of Pakistan (Detail of Fig.3) (TK = mostly Eocene nummulitic limestone, Cretaceous limestone and mostly Giumal sandstone; K = mostly limestone and Giumal sandstone).

opposite page
Fig. 5
Geologic and Mineral Resource Map of Afghanistan by U.S. Geological Survey 2006 (detail).

geological formations (Fig. 5). In particular, in the area of Ghazni (where Tapa Sardar is situated), we note the presence of Pleistocenic continental deposits, composed by alluvium and colluvium, loess deposits, conglomerate, and Triassic sandstone and siltstone.

In the Fundukistan area, north of Kabul, we note the presence of: grey schist and phyllite of the Neoproterozoic age; sandstone and siltstone of the Carboniferous-Permian age; limestone and dolomite of Late Triassic and Early Triassic; Miocenic conglomerate and sandstone; gray conglomerate and sandstone more abundant in siltstone, clay and limestone from Pliocene.

The southern area of Kabul (where Mes Aynak, Hadda and Tepe Narenj are located), shows the presence of gneiss (Paleoproterozoic), marble and quartzite Cambrian and Neoproterozoic, limestone and dolomite Middle and Early Triassic, sandstone and siltstone Late and Middle Triassic, ultramafic intrusions (dunite, peridotite and serpentinite of Eocene), Pliocenic conglomerate and sandstone, alluvial conglomerate and sandstone of

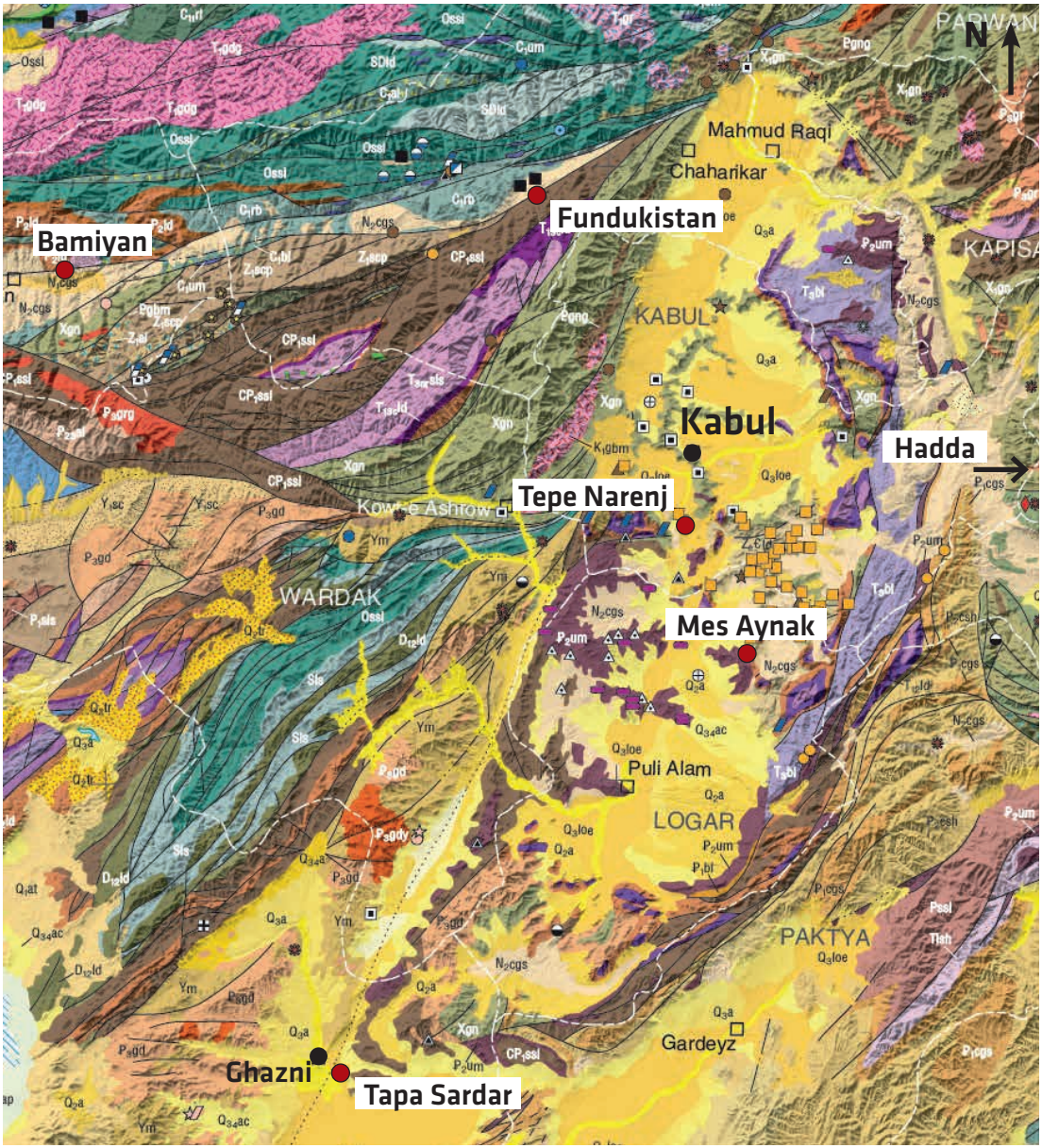

$Q_{34}ac$ **Fan alluvium and colluvium (Holocene and late Pleistocene)**—Fan alluvium and colluvium: shingly and detrital sediments, gravel, sand, clay

Q_3a **Conglomerate and sandstone (late Pleistocene)**—Alluvium: shingly and detrital sediments, gravel, sand more abundant than silt and clay

Q_3loe **Loess (late Pleistocene)**—Loess more abundant than sand, clay

Q_2a **Conglomerate and sandstone (middle Pleistocene)**—Alluvium: shingly and detrital sediments, gravel, sand more abundant than silt and clay

N_2cgs **Conglomerate and sandstone (Pliocene)**—Gray conglomerate, grit, sandstone more abundant than siltstone, clay, limestone, marl; gypsum, salt; felsic to mafic volcanic rocks

P_3ssl **Sandstone and siltstone (Oligocene)**—Sandstone, siltstone more abundant than clay, conglomerate, limestone, marl; felsic and mafic volcanic rocks

P_3gdy **Granodiorite and granosyenite (Oligocene)**—Granodiorite, alaskite, granosyenite more abundant than granite (Phase II)

P_1cgs **Conglomerate and sandstone (Paleocene)**—Conglomerate, sandstone more abundant than siltstone, limestone, shale; mafic volcanic rocks

P_1bl **Basalt lava (Paleocene)**—Basalt lava

K_1gbm **Gabbro and monzonite (Early Cretaceous)**—Gabbro, monzonite more abundant than diorite, granodiorite

Tlsh **Limestone and shale (Triassic)**—Limestone, shale more abundant than sandstone

T_3sab **Sedimentary and volcanic rocks (Late Triassic)**—Shale more abundant than phyllite, andesite to basalt (greenstone altered), limestone (Kotagai series)

T_3rl **Rhyolite (Late Triassic)**—Rhyolite lava

T_3bl **Basalt lava (Late Triassic)**—Basalt lava

$T_{1c}ld$ **Limestone and dolomite (Late Triassic (Carnian) and Early Triassic)**—Limestone, dolomite more abundant than conglomerate, chert, marl (Middle Afghanistan); limestone, sandstone, shale, conglomerate, chert, mafic volcanic rocks (Khashrud zone); limestone, dolomite (Kismaran zone)

C₁rb **Volcanic and sedimentary rocks (Early Carboniferous)**—Rhyolitic to basaltic volcanic rocks more abundant than limestone, slate, sandstone, conglomerate

SDld **Limestone and dolomite (Devonian and Silurian)**—Limestone and dolomite more abundant than schist, sandstone

Sls **Limestone (Silurian)**—Limestone, marl more abundant than slate

Ossl **Sandstone and siltstone (Ordovician)**—Sandstone and siltstone more abundant than shale (Logar and Argandab zones); limestone, sandstone, siltstone, shale (Middle Afghanistan); shale, sandstone, chert (North Afghanistan)

X_2vl **Metavolcanic lava (middle Paleoproterozoic)**—Metavolcanic lava

X₂gn **Gneiss (early Paleoproterozoic)**—Two-mica, biotite, biotite-amphibole, garnet-biotite, garnet-sillimanite-biotite, pyroxene-amphibole, plagioclase, and cordierite gneisses; schist, migmatite, quartzite, marble, amphibolite

Xgn **Gneiss (Paleoproterozoic)**—Two-mica, biotite, biotite-amphibole, garnet-biotite, and plagioclase gneisses; migmatite, quartzite, marble, amphibolite

Ym **Metamorphic rocks, undifferentiated (Mesoproterozoic)**—Greenschist, gneiss, quartzite, marble, amphibolite (metavolcanic lava and sedimentary rocks)

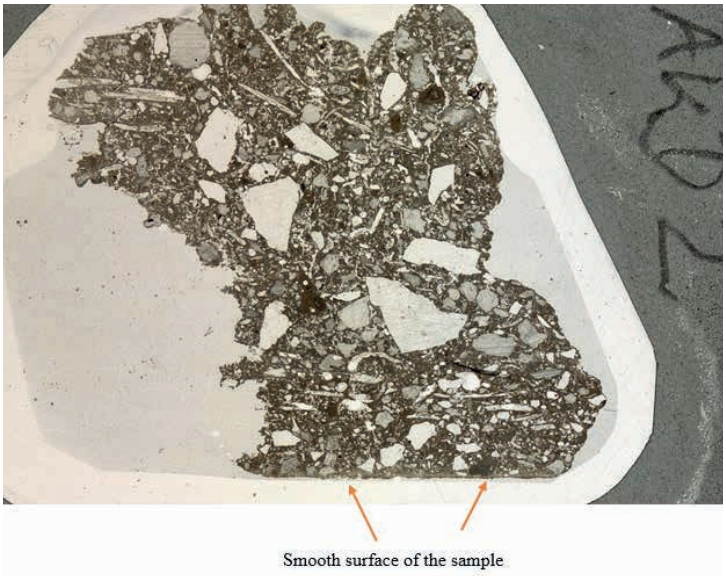

Fig. 6
Cross section of sample AKD 2 from Amluk-dara, Pakistan (image is 37 mm across).

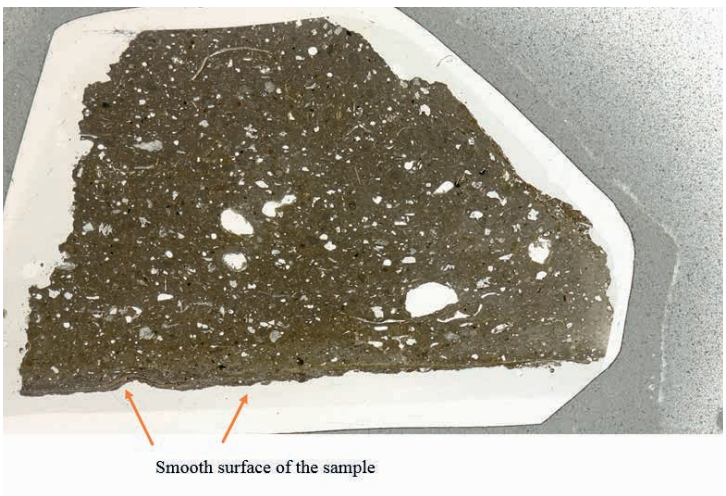

Fig. 7
Cross section of sample AKD 4 from Amluk-dara, Pakistan (image is 37 mm across).

the Middle and Late Pleistocene, alluvial and colluvial fan (Late Pleistocene and Holocene).
(C.R., S.P.)

Petrographic analysis of Gandharan stucco samples from Pakistan
Sample AKD 2
This sample was taken from a stucco architectonical decoration of a building in Amluk-dara archeological site.
Through a petrographic microscope analysis we noted that the large white grains are angular fragments of quartzite, whereas grey colored grains are mainly fragments of single crystals of calcite, probably originating from coarse marble (Fig. 6). The fine-grained binder matrix consists of calcite

appears brownish (note the smooth surface at the bottom of the image). Fragments of a smooth surface layer are preserved. This is mainly composed by fine-grained sheet silicates and some larger mica flakes. Small quartz grains are also present.
As the microscopic study shows, the surface layer derives from a smoothing, because the original one was rough, owing to the presence of coarse-grained components in the stucco, such as quartzite or calcite grains. It can also be expected that the original surface was somehow shiny, due to the presence of coarser mica flakes.

Sample AKD 4
This sample was taken from a stucco architectonical decoration of a building in Amluk-dara archeological site.
Through a petrographic microscope analysis we noted that intermediate size white grains are angular fragments of quartzite; the grey colored grains are mainly fragments of single crystals of calcite probably originating from coarse marble. The fine-grained binder matrix, mainly consisting of calcite, appears brownish (Fig. 7).
Fragments of a smooth surface layer are also preserved. This is mainly composed by fine-grained sheet silicates ('clay') and of some larger mica flakes. Small quartz and tourmaline grains are also present. Interesting results also came from microprobe analysis, about the presence and the amount of calcite (Fig. 8).
On the surface we observed three layers: a very thin (c. 2 µm) red brownish layer is covered by a fine-grained ochre layer, covered by a dirty layer rich of sheet silicates, mica flakes and quartz grains (and tourmaline) (Fig. 9).

Sample AKD 5
This sample was taken from a stucco architectonical decoration of a building in Amluk-dara archeological site.
Through petrographic microscope analysis we noted that the sample contains centimetric angular fragments of quartzite, granite, gneiss, garnet, and marble. In addition, mica flakes are present. The fine-grained binder matrix, mainly consisting of calcite, appears brownish (Fig. 10).
The surface layer is composed of fine-grained sheet silicates ('clay') and some larger mica flakes. Small quartz grains are also present.
This layer is separated from the stucco by a 20 µm thick sheet of fibrous calcite with fiber axis perpendicular to the surface. This layer could represent the product of a water-lime suspension painted into the stucco surface.

Sample AKD 14C
This sample was taken from a stucco architectonical polychrome decoration of a building in Amluk-dara archeological site.
Through a petrographic microscope analysis we noted that the stucco in this sample has been made using a lime mortar. The added rock fragments

Fig. 8 a, b, c
Sample AKD 4 from Amluk-dara, Pakistan (back-scattered electron image). The surface layer consists of mica flakes that are aligned parallel to the surface. Quartz and titanite grains are present as well. Spots 2 to 5 are mainly composed of calcite with smaller amount of Al and Si (see spectra 2 to 5) probably resulting from a small portion of clay minerals.

mainly consist of angular rock compounds, up to 2 mm in size. The grain size spectrum is continuous (Fig.11).
The stucco contains mm-sized angular fragments of quartzite, granite, gneiss, garnet, and marble. In addition, mica flakes are present in the fine-grained matrix. The fine-grained binder matrix, mainly consisting of calcite, appears brownish (Fig. 12).
Fragments of a smooth surface layer are preserved. The layer rested on a smooth surface of the stucco material. The layer itself is composed by two sublayers: an inner one is a thin reddish layer (0.01 mm thick). This inner layer is covered by an outer layer that contains a large amount of fine-grained material (binder ?) and some larger mica flakes. The red colour results hematite (c. 2 µm) by Raman analysis (Figg. 13, 14). Partly, the surface of the sample is covered by a layer of dirt rich in fine grained sheet silicates and calcite.

Sample AKD 13C
This sample was taken from a stucco architectonical polychrome decoration of a building in Amluk-dara archeological site.
This sample is a fragment of an architectural decoration in stucco, made using lime mortar (fig. 15). Petrographic microscope analysis and Electron Microprobe analyses highlighted that the matrix contains a great amount of calcite (Figg. 16, 17, 18).
The added rock fragments mainly consist of angular rock compounds up to 7 mm in size. The grain size spectrum is continuous. Rock fragments comprise high-grade metamorphic rocks, plutonic rocks and marble. The region of provenance is probably an heterogeneous basement area. Some rock fragments of garnet micaschist are composed of a large, mm sized garnet, with attached mica rich country rock. Such aggregates are unstable in the sedimentary process. It is therefore evident that the rocks were artificially crushed to produce the lime mortar.

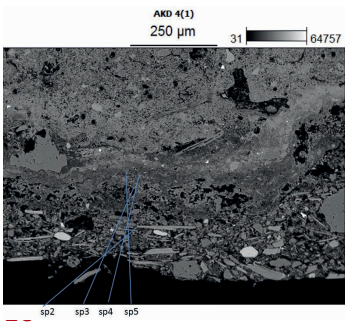

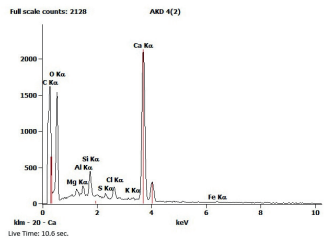

Acc.Voltage: 15.0 kV Take Off Angle: 40.0 deg.
Quantitative Results for: AKD 4(2)

Element	Weight %	Weight % Error	Atom %	Compd %
O	30.965	---	51.92	---
Mg	1.02	+/- 0.08	1.13	1.69
Al	1.23	+/- 0.08	1.22	2.32
Si	3.55	+/- 0.14	3.39	7.60
S	0.80	+/- 0.08	0.67	2.00
Cl	2.40	+/- 0.17	1.81	2.40
K	0.33	+/- 0.09	0.23	0.40
Ca	57.96	+/- 0.55	38.79	81.10
Fe	1.74	+/- 0.30	0.84	2.49
Total	100.00		100.00	100.00

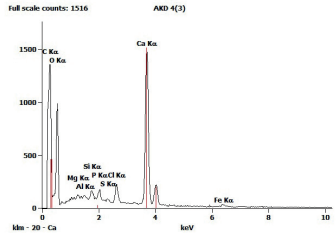

Acc.Voltage: 15.0 kV Take Off Angle: 40.0 deg.
Quantitative Results for: AKD 4(3)

Element	Weight %	Weight % Error	Atom %	Compd %
O	29.805	---	51.01	---
Mg	0.67	+/- 0.10	0.75	1.11
Al	0.67	+/- 0.09	0.68	0.89
Si	1.38	+/- 0.10	1.34	2.94
P	1.75	+/- 0.11	1.55	4.01
S	0.38	+/- 0.09	0.32	0.94
Cl	4.32	+/- 0.23	3.34	4.32
Ca	57.93	+/- 0.65	39.59	81.06
Fe	3.31	+/- 0.43	1.62	4.73
Total	100.00		100.00	100.00

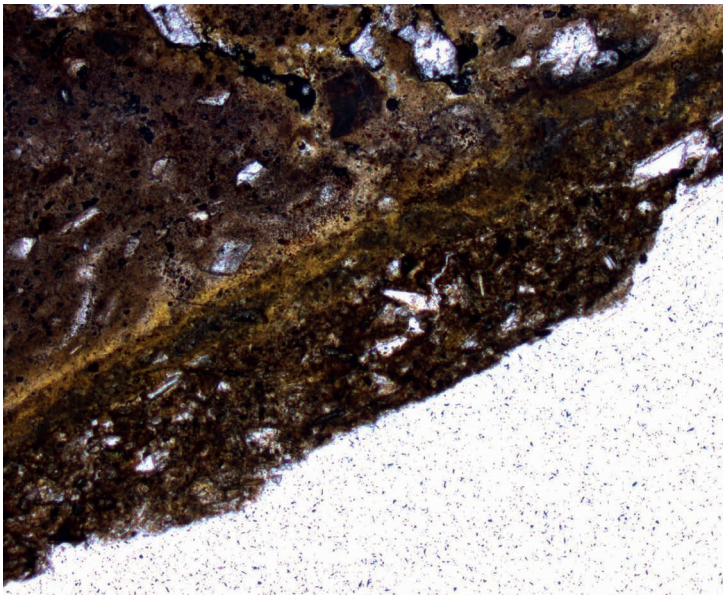

Fig. 9
Sample AKD 4 from Amluk-dara, Pakistan (image is 1.8 mm across).

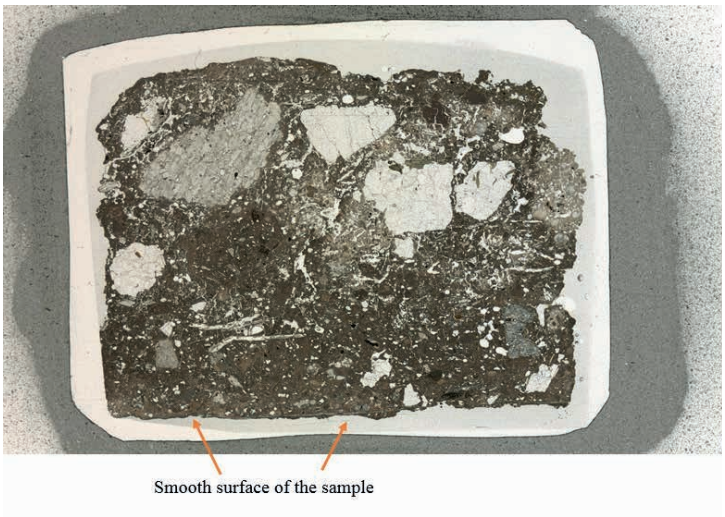

Fig. 10
Cross section of sample AKD 5 from Amluk-dara, Pakistan (image is 37 mm across). Note the smooth surface at the bottom of the image.

XRD analyses on sample AKD 14C and AKD 13C show a similar chemical composition of the stucco material, with a high presence of calcite (Fig. 19).

Sample BKG 1123 16C

This sample was taken from a stucco architectonical polychrome decoration of a building in Barikot archeological site.

The sample BKG 1123 16C consists in stucco produced from a lime mortar. The added rock fragments mainly consist of angular rock compounds up to 1 mm in size. The grain size spectrum is continuous (Fig. 20).

opposite page

Fig. 11
Sample AKD 14C of architectonical polycrome decoration from Amluk-dara, Pakistan (photo E. Loliva ©ISCR).

Fig. 12
Cross section of sample AKD 14C from Amluk-dara, Pakistan (image is 37 mm across). Note the original smooth surface on the right side of the image. Remnants of reddish color are visible there.

Fig. 13
Sample AKD 14C from Amluk-dara, Pakistan (petrograpich microscope image is 1.8 mm across-1 polar). Detail of the partly preserved smooth surface layer.

The added rock and mineral fragments mainly indicate a sedimentary origin (limestones). Only a few fragments come from some relatively high metamorphic or igneous rocks. Angular fragments mainly consist of quartz and limestone. The grain size distribution is serial with a few fragments of more than 1 mm in size. Fragments are embedded in a brownish, fine-grained matrix representing the former lime mortar. The grain size distribution of added fragments is mainly in sand fraction or finer (Fig. 21). Enlarged view of the mortar matrix mainly composed of tiny calcite crystals (Fig. 22).

The EDS analyses reveal that the mortar attached to the rock fragments mainly contains Ca, as due to the calcite content. Additional elements found in the rock fragments contain Na, K, Ca, Mg, Fe, Al, and Si. These elements can be related to various minerals such as plagioclase, K-feldspar, muscovite, biotite, and garnet (Figg. 23, 24). On the surface of the sample we recognise a few traces of very pale, faint and dilute red colour that it was not possible to analyze in this research.

Sample BKG 1123 15C

This sample was taken from a stucco architectonical polychrome decoration of a building in Barikot archeological site.

Sample BKG 1123 15C is a stucco, made using a lime mortar. The added rock fragments mainly consist of angular rock compounds up to 6 mm in size. The grain size spectrum is serial continuous. Added rock and mineral fragments mainly indicate a relatively high metamorphic origin (Fig. 25). By means of a petrographic microscope we note some irregular pore spaces (shrinking cracks ?) in the fine grained brownish matrix (Fig. 26). The sample contains rock fragments of a relatively high-grade metamorphic rock, containing minerals such as feldspar, muscovite, biotite, margarite, tourmaline, and garnet. These minerals are embedded in a fine-grained binder mainly composed of calcite.

EDS analyses of the binder indicate that, in addition to calcite, elements such as Si, Al, K and S are present. This could point to a certain fraction of clay added to the binder of the stucco mixture.

Fig. 14
Sample AKD 14C from Amluk-dara, Pakistan. Raman spectrum of the thin red layer (red) compared with a pure hematite spectrum (blue).

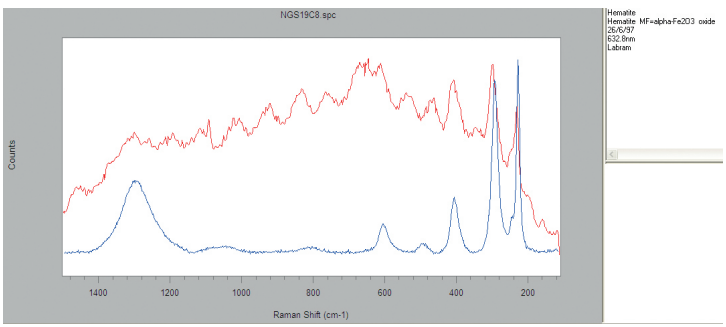

On the surface of the sample a few traces of very pale, faint and diluted red color were observed, though it was not possible to analyze them, we hope to do it in next future.

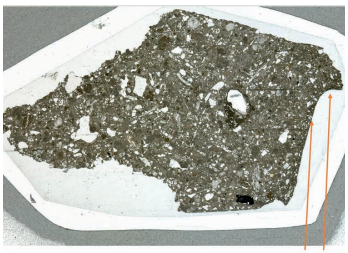
Original smooth surface of the sample with remnants of red colo

Sample GBK 17A

This sample was taken from a stucco architectonical polychrome decoration of a building in Gumbat archeological site.

By petrography analysis we highlighted that the sample GBK 17A is a stucco made using lime mortar. The added rock fragments mainly consist of limestones up to 1 mm in size and, to a lesser extent, of quartz grains. The grain size spectrum is serial continuous. The added rock and mineral fragments mainly indicate a sedimentary origin (limestones). Only a few fragments come from relatively high metamorphic or igneous rocks. A surface layer has a different composition if compared to the bulk sample. The surface layer contains a higher fraction of mica flakes (Fig. 27).

In addition, irregular pores are visible (possibly partly artificially created during preparation). The origin of a thin, curved pore is not clear (Fig. 28), fibre-like pore structures have an unknown origin (Fig. 29). The surface layer of the sample is composed by much finer grained material. The surface layer is about 0.6 mm thick (Fig. 30). By Electron microprobe analyses the bulk sample is mainly composed by fragments of limestone with a few fragments of relatively high-grade metamorphic rock (Fig. 31).

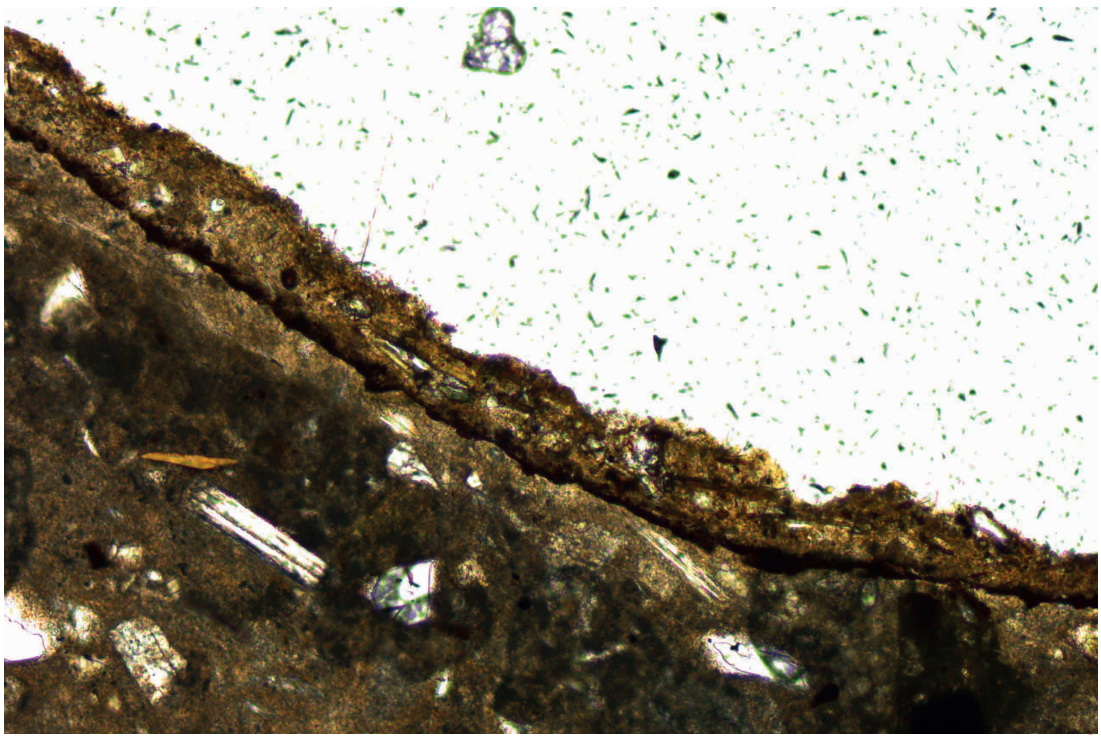

Fig.15
Sample AKD 13C of architectonical decoration from Amluk-dara, Pakistan (photo E. Loliva ©ISCR).

Fig.16
Thin section of sample AKD 13C from Amluk-dara, Pakistan (image is 37 mm across). Large rock fragments partly consist of micaschists that contain mm-sized garnet crystals.

These minerals are embedded in a fine-grained binder, mainly composed of calcite. EDS analyses of the binder indicate that, in addition to the calcite, elements such as Si, Al, K and S are present. This element could point to a certain fraction of clay added to the binder. A surface layer has a different composition: it contains a high fraction of metamorphic minerals such as feldspar, muscovite, garnet, and chloritoid. Furthermore, XRD analysis pointed out that the surface layer contains much more feldspar, mica, and calcite than the bulk sample.

Sample of 'Kanjur'

This fragment of 'kanjur' rock is a sample of building material taken in an archaeological excavation in Amluk-dara site (Swat) (Fig. 32). Petrographical analysis higlighted that this sample is an organogenic limestone, mainly composed of calcite. A prominent feature of this rock is a porous microstructure (Fig. 33). Furthermore, spherical structures and pagoda-like structures characterized by a central void (marked by arrows) are visible. The rock was probably originate by a colony of calcareous porifera or calcareous algae in a marine environment (ancient Tethis sea). Such a rock may be classified as a biocalcarenite. The rock can easily be cut and shaped. In addition, the rough surface of the porous rock is decorative and may be used for ornamental purposes.

By an analysis of the microstructure of the rock we noted a cone-like structure of calcite sheets with a central channel (Fig. 34). Moreover, relatively closely packed structure of spheroidal shape are present (Fig. 35).

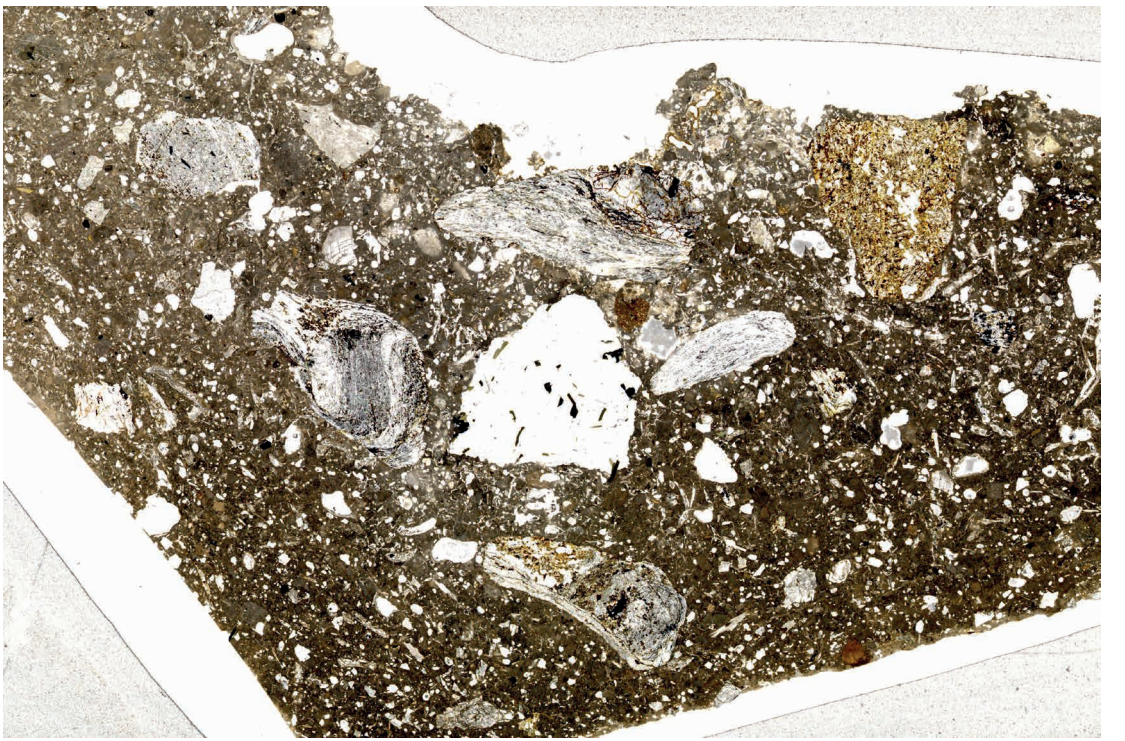

Then, back scattered electron images are used to document the microstructure of the samples. Compared to transmitted light images, the resolution is higher because only the polished surface of the samples is displayed (Figg. 36, 37).
For the phase analysis, X-ray diffraction techniques were also applied. It can be confirmed that calcite is the main phase of this sample of stone. No other mineral can be detected (Fig. 38).
(T. T)

Petrographic analysis on the Gandharan clay samples from Afghanistan

Sample 1 from Tapa Sardar, Afghanistan

Sample 1 is a fragment of a relatively hard and solid fired clay artefact (Fig. 39). By a petrographic microscope analysis we noted that the color is red, with 0.5 to 1 mm sized, bright sand components, visible to the naked eye (Fig. 40). It contains sand fragments that are angular shaped minerals (feldspar, quartz) and rock fragments (phyllite, limestone, quartzite) (Fig. 41). A natural clay served as a binder. Chemical analyses of sheet silicates show that particularly biotite was oxidized during the burning process. Remnants of clay minerals are characterized by low totals and also oxidized during the burning process. The rock and mineral fragments can derive from sedimentary rocks (limestone) or from crystalline rocks (hornblende, K-feldspar, garnet). The compositions of the latter ones conform to a medium to high grade metamorphic basement.
In addition to the petrographic microscope, the microstructure of this sample was analyzed with an electron microprobe. The chemical composition of the minerals is measured with the same machine, employing wavelength dispersive techniques.

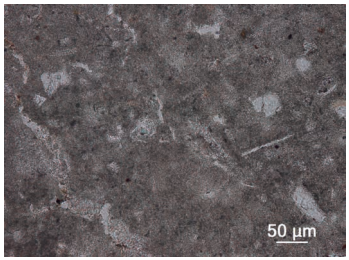

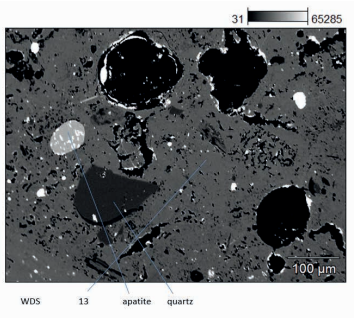

Fig.17
Sample AKD 13C from Amluk-dara, Pakistan (petrographic microscope image: 1 polar). The fine-grained brownish matrix is composed of µm-sized calcite crystals.

Fig. 18
Sample AKD 13C from Amluk-dara, Pakistan. Back-scattered electron image, 13 calcite: fine-grained matrix with mica flake and pore space (black).

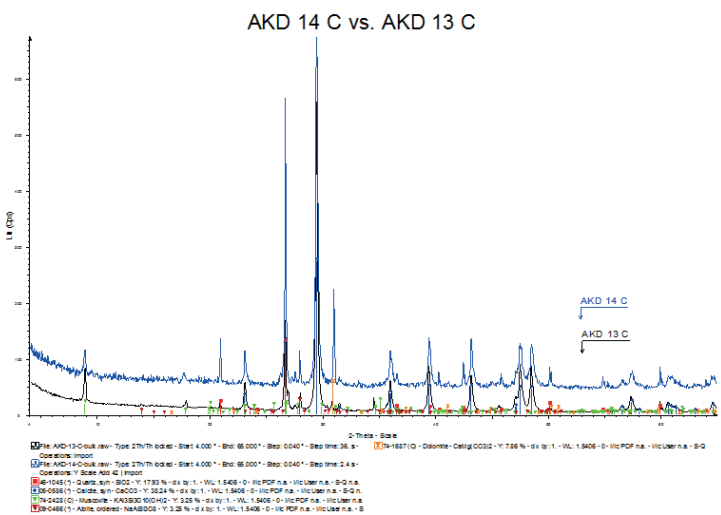

Fig. 19
X-ray diffraction (XRD) analyses on samples AKD 14C and AKD 13C from Amluk-dara, Pakistan.

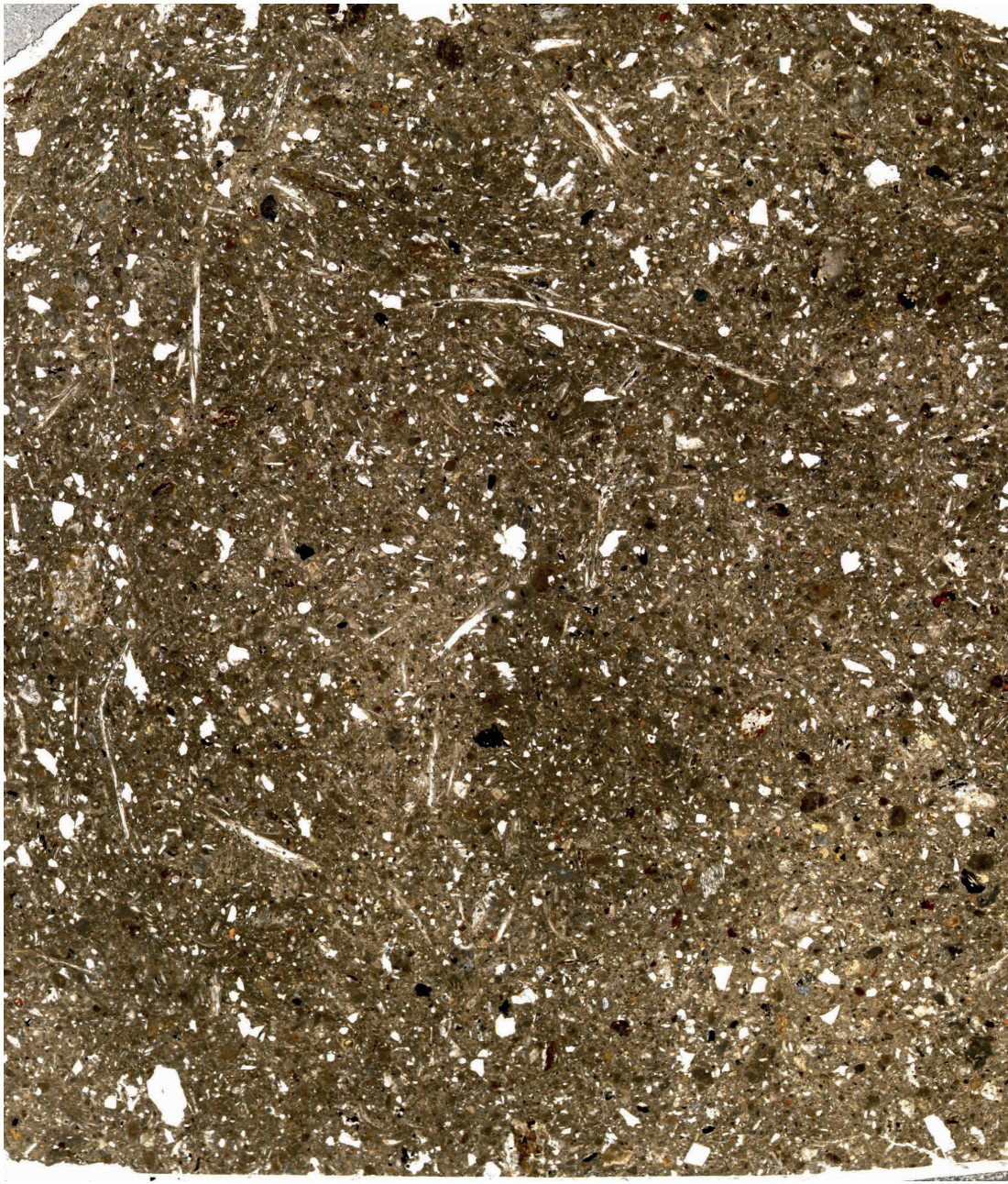

The black colour on the surface of this sample was so far not found to have a chemical characterisation (Fig. 42).
Moreover, by an X-ray diffractogram analysis of this sample the following phases were recognized: quartz, plagioclase (albite), K-feldspar, hornblende, and muscovite (Fig. 43).

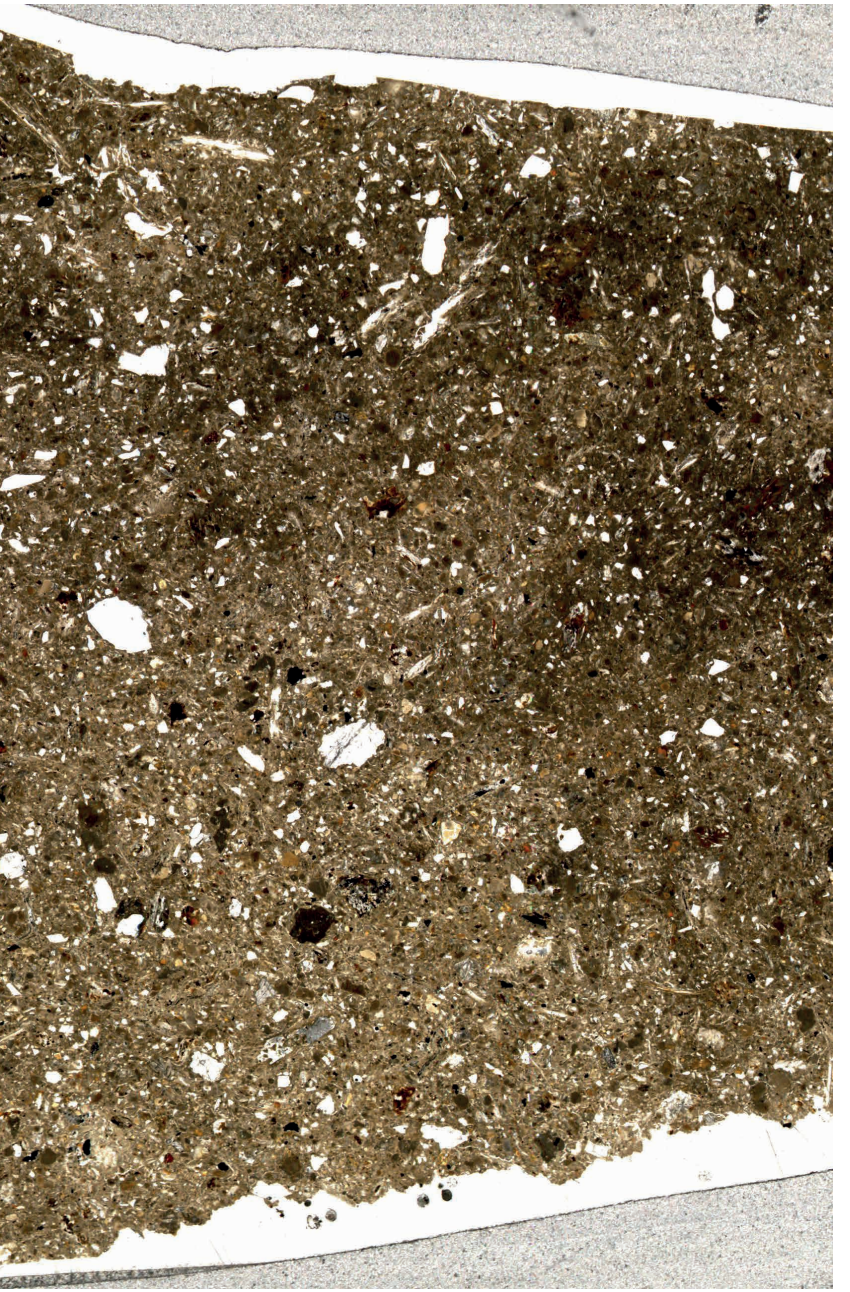

Fig. 20
Thin section of sample BKG 1123 16C from Barikot, Pakistan (image is 37 mm across).

Fig. 21
Sample BKG 1123 16C from Barikot, Pakistan (petrographic microscope image: image is 7 mm across - 1 polar).

Fig.22
Sample BKG 1123 16C from Barikot, Pakistan (petrographic microscope image: image is 0.45mm across - 1 polar).

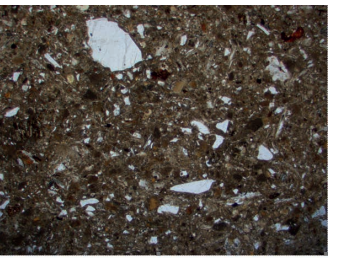

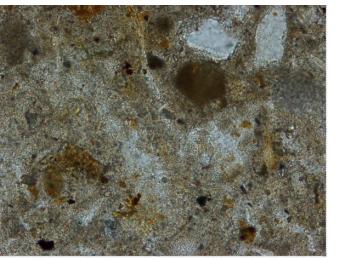

Sample 2 from Tepe Narenj, Afghanistan

Sample 2 is a fragment of a relatively soft fired clay artefact (Fig. 44), which tends to disintegrate during the handling. The color is red with 0.5 to 1 mm size, bright sand components are visible to the naked eye. By petrographic microscope analysis we highlighted that it contains sand fragments consisting in angular shaped minerals (feldspar, quartz) and rock fragments

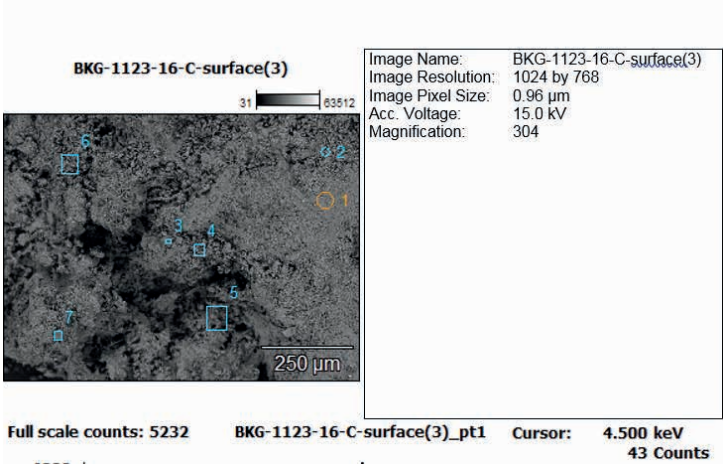

Fig. 23
Sample BKG 1123 16C from Barikot, Pakistan. Electron Microprobe analyses (WDS): surface of the sample.

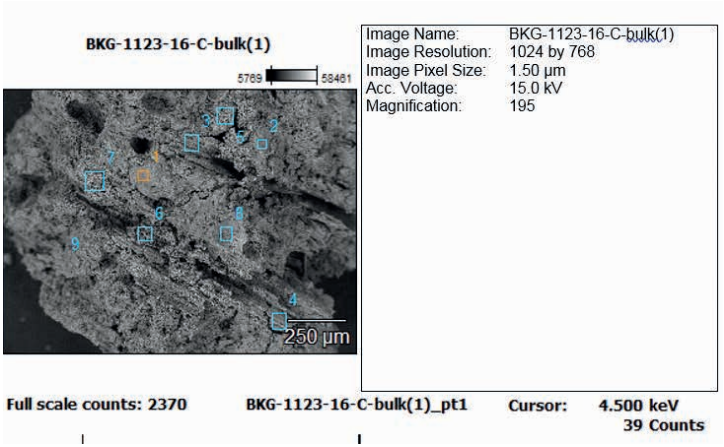

Fig. 24
Sample BKG 1123 16C from Barikot, Pakistan. Electron Microprobe analyses (WDS): bulk of the sample.

Fig. 25
Thin section of sample BKG 1123 15C from Barikot, Pakistan. Petrographic microscope image: image is 37 mm across.

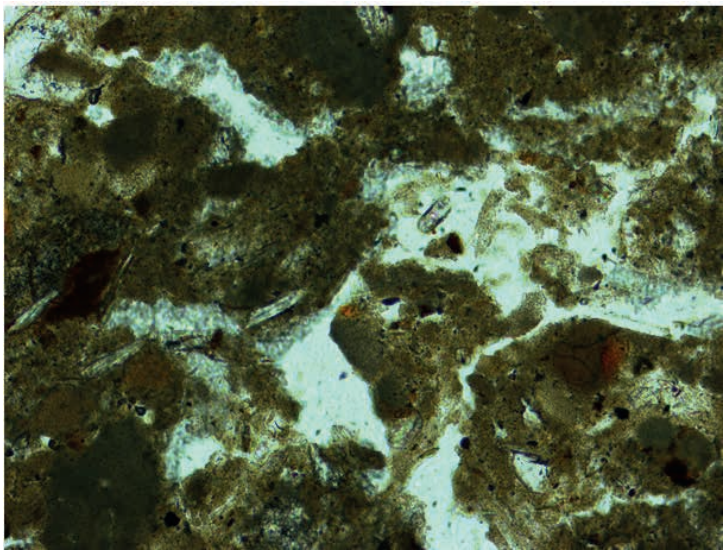

Fig. 26
Sample BKG 1123 15C from Barikot, Pakistan (image is 0.9 mm across - 1 polar). Petrographic microscope image: view of irregular pore space (shrinking cracks ?) in the fine grained brownish matrix.

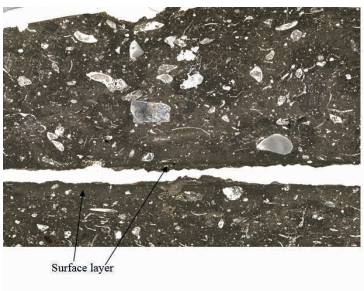

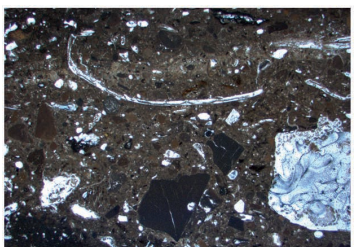

Fig. 27
Thin section of sample GBK 17A from Gumbat, Pakistan (image is 37 mm across).

Fig. 28
Sample GBK 17A from Gumbat, Pakistan (image is 7 mm across - 1 polar). Petrographic microscope image: an overview of the sample shows angular rock fragments in a fine grained matrix.

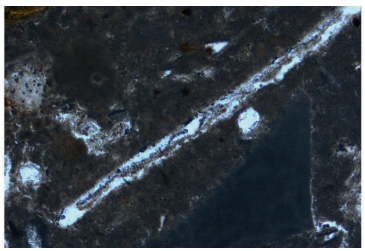

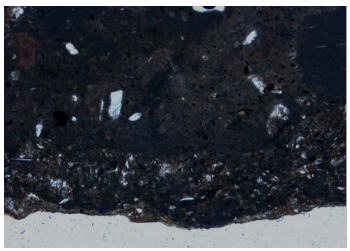

Fig. 29
Sample GBK 17A from Gumbat, Pakistan (image is 0.9 mm across -1 polar). Petrographic microscope image: a fibre-like pore structure of unknown origin and, at the bottom of the image, a fragment of limestone embedded in a matrix of fine grained calcite is visible.

Fig. 30
Sample GBK 17A from Gumbat, Pakistan (image is 1.8 mm across -1 polar). Petrographic microscope image: the surface layer (facing down) is composed by much finer grained material compared to the bulk sample.

(phyllite, limestone, quartzite). A natural clay and fine-grained calcite served as binders (Fig. 45).

The peculiarity of the sample is that relatively large single crystals of gypsum are in the sand fraction. Because gypsum is thermally not stable during a normal, high temperature burning process, it can be concluded that this mineral is either the result of a secondary process or the temperature of the burning process was very low (Fig. 46).

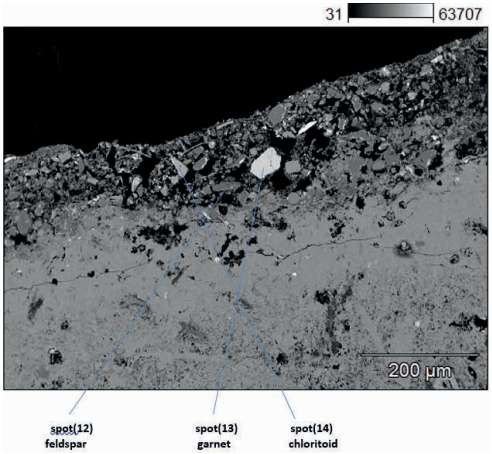

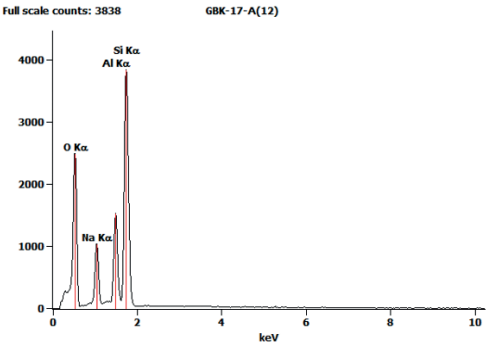

Live Time: 5.1 sec.

Acc.Voltage: 15.0 kV Take Off Angle: 40.0 deg.
Quantitative Results for: GBK-17-A(12)

Element	Weight %	Atom %	Compnd %
O	49.005	61.76	---
Na	8.31	7.29	11.21
Al	10.11	7.56	19.11
Si	32.57	23.39	69.68
Total	100.00	100.00	100.00

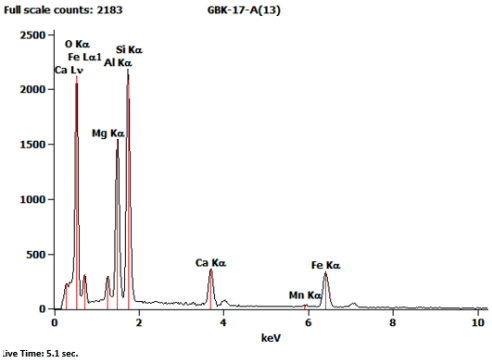

ive Time: 5.1 sec.

cc.Voltage: 15.0 kV Take Off Angle: 40.0 deg.
uantitative Results for: GBK-17-A(13)

Element	Weight %	Atom %	Compnd %
O	42.335	61.81	---
Mg	1.71	1.65	2.84
Al	11.06	9.58	20.90
Si	17.44	14.51	37.32
Ca	5.93	3.46	8.30
Mn	0.86	0.37	1.11
Fe	20.65	8.64	29.52
Total	100.00	100.00	100.00

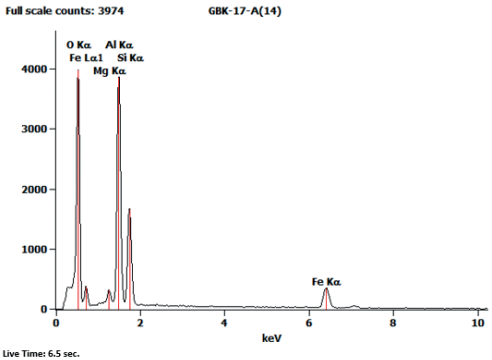

Live Time: 6.5 sec.

Acc.Voltage: 15.0 kV Take Off Angle: 40.0 deg.
Quantitative Results for: GBK-17-A(14)

Element	Weight %	Atom %	Compnd %
O	43.625	61.74	---
Mg	1.28	1.20	2.13
Al	22.61	18.97	42.71
Si	12.28	9.90	26.27
Fe	20.21	8.19	28.89
Total	100.00	100.00	100.00

Fig. 31 a, b, c, d

Sample GBK 17A from Gumbat, Pakistan. Electron Microprobe analyses (WDS): detail of fine-grained minerals in the surface layer. Note the presence of mica, feldspar, and garnet. Spot 12, 13 and 14: EDS analysis of the fine-grained matrix.

Chemical analyses of sheet silicates show that most of them were altered during the burning process. The analyzed compositions are particularly rich in Ca, in contrast with the naturally occurring ones. The rock and mineral fragments could derive from sedimentary rocks (limestone) or from crystalline rocks (hornblende, K-feldspar, garnet). The composition of the latter ones, conform to a medium to high grade metamorphic basement (Fig. 47). The composition of hornblende in this sample is different from the one in the sample from Tapa Sardar, indicating a different region of provenance of the sand.

Fig. 32
Sample of 'kanjur' rock (photo T. Theye).

By an X-ray diffractogram analysis the following phases can be recognized: quartz, plagioclase (albite), K-feldspar, hornblende, muscovite, calcite, and gypsum (Fig. 48)
(T.T., C.R.)

Conclusions

The Gandharan archaeological sites are mostly located in the Indus Suture Zone (see above, n.2) and in the lower Swat (see above n.1). In a recent past, scholars observed the use of local different type of schists to build buildings and sacred artworks[10]. In this new research we highlighted the use of limestone for stucco artefacts and architectural decorations. This limestone is not a local rock in Swat (see above) but its main, extended and closer outcrops are located in the mountains northwest of Islamabad. Indeed, through specific analyses carried out by our team, the compatibility of these outcrops with the rocks used for stucco artefacts and stucco decorations of buildings was observed[11]. This stucco was made by a mixture of different kinds of local crushed rocks (i.e. schists and granites).

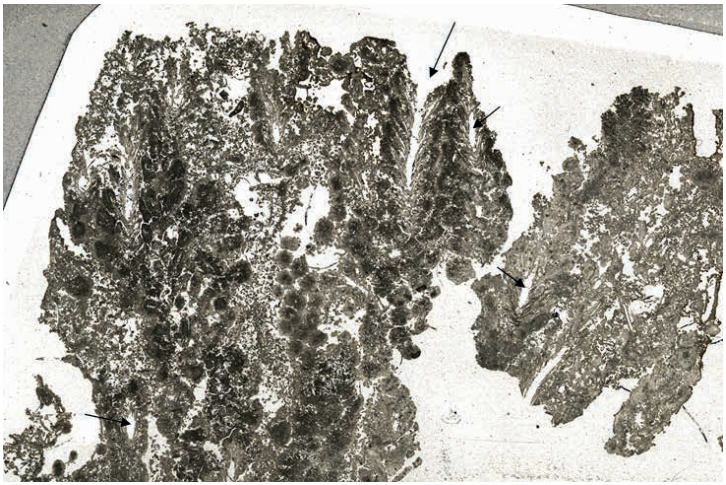

Fig. 33
Polished thin section of 'kanjur' rock, overview: a prominent feature of this rock is a porous microstructure (white areas in the image) (image is 3.5 cm across).

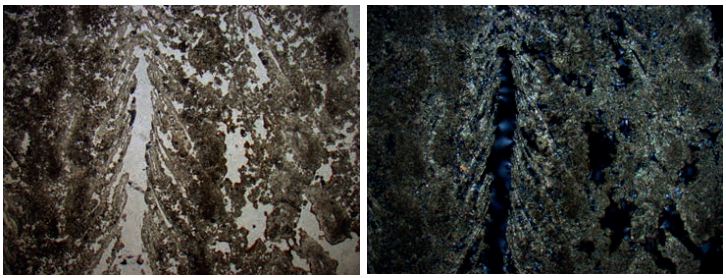

Fig. 34
Sample of 'kanjur' rock, analysis of the microstructure: cone-like structure of calcite sheets with a central channel. Petrographic microscope image: left image: 1 polar; right image + polars (images are 6.8 mm across).

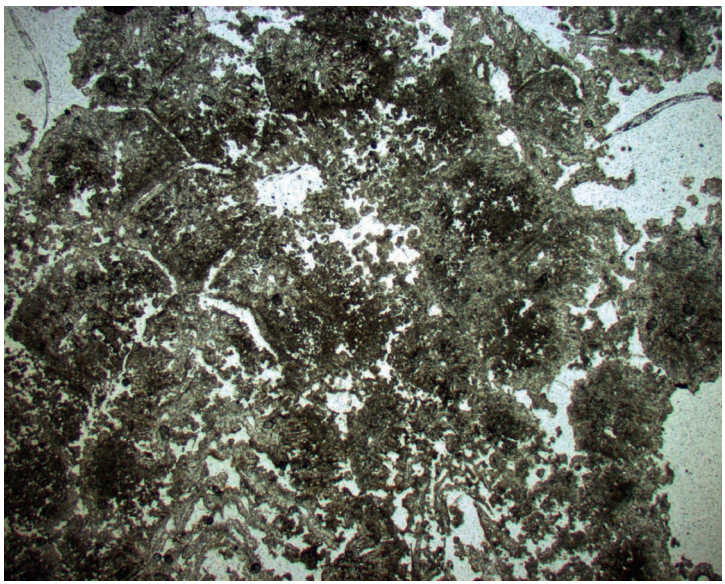

Fig. 35
Sample of 'kanjur' rock, analysis of the microstructure: relatively closely packed structure of spheroidal shapes (petrographic microscope image is 6.8 mm across – 1 polar).

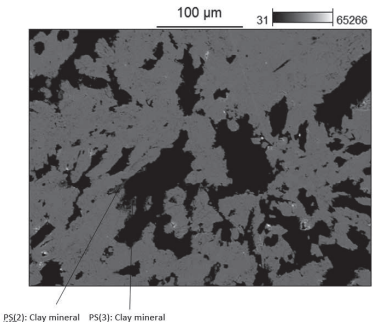

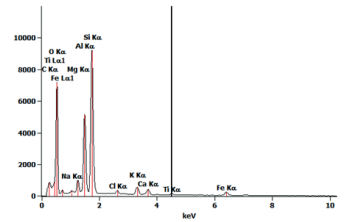

Acc.Voltage: 15.0 kV, Take Off Angle: 40.0 deg.
Quantitative Results for: Sample1-C1(2)

Element	Weight %	Atom %	Atom % Error	Compnd %
O	46.805	62.42	+/- 0.70	---
Na	0.45	0.41	+/- 0.04	0.60
Mg	1.97	1.73	+/- 0.06	3.26
Al	12.16	9.62	+/- 0.09	22.99
Si	26.55	20.17	+/- 0.11	56.81
Cl	0.97	0.58	+/- 0.04	0.97
K	2.76	1.51	+/- 0.03	3.32
Ca	2.16	1.15	+/- 0.03	3.02
Ti	0.83	0.37	+/- 0.02	1.38
Fe	5.35	2.05	+/- 0.10	7.65
Total	100.00	100.00		100.00

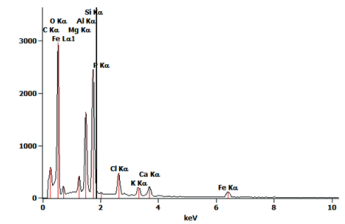

Acc.Voltage: 15.0 kV, Take Off Angle: 40.0 deg.
Quantitative Results for: Sample1-C1(3)

Element	Weight %	Atom %	Atom % Error	Compnd %
O	45.285	60.07	+/- 0.67	---
Mg	2.24	2.05	+/- 0.11	3.72
Al	11.70	9.65	+/- 0.15	22.11
Si	22.53	17.66	+/- 0.18	47.78
P	0.52	0.23	+/- 0.04	0.72
Cl	5.39	3.38	+/- 0.10	5.39
K	2.98	1.69	+/- 0.05	3.59
Ca	3.96	2.20	+/- 0.06	5.55
Fe	7.80	3.10	+/- 0.22	11.15
Total	100.00	100.00		100.00

Fig. 36 a, b, c
Sample of 'kanjur' rock. Back-scattered electron image. Impurities in the calcite structure consisting of tiny particles of clay mineralswhich appears darker than calcite. EDS spectrum and elemental composition of clay fragments. Chlorine may be contributed by the resin (araldite).

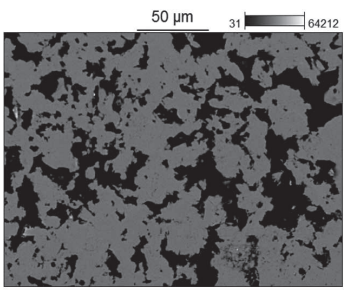

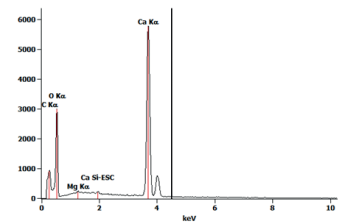

Acc.Voltage: 15.0 kV, Take Off Angle: 40.0 deg.
Quantitative Results for: Sample1-D1(5)

Element	Weight %	Atom %	Atom % Error	Compnd %
O	28.585	50.00	+/- 0.49	---
Mg	0.26	0.30	+/- 0.05	0.43
Ca	71.16	49.70	+/- 0.30	99.57
Total	100.00	100.00		100.00

Fig. 37 a, b
Sample of 'kanjur' rock. Back-scattered electron image. Detail of the core of the spheroidal particle: most of the calcite shows euhedral crystal faces. EDS spectrum and elemental composition of calcite: note the presence of small amount of Mg in calcite.

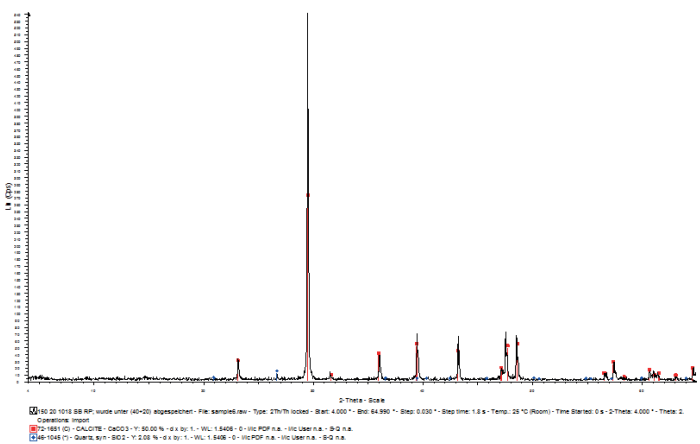

Fig. 38
Sample of 'kanjur' rock. X-ray diffraction (XRD) analysis.

Fig. 39
Sample 1 of clay artefact from Tapa Sardar, Afghanistan. Close-up of sample. Bright, mm sized sand fragments embedded in a reddish matrix are visible (photo T. Theye).

We therefore suppose that the limestone was transported from these sites to Swat mainly by road paths and perhaps through water ways.
The study of the geological outcrops shows a great difference between the area of Gandharan sites in Pakistan and the Afghanistan ones. In Pakistan we mainly note the presence of metamorphic rocks, whereas in Afghanistan, of limestone, sandstone and siltstone, attributed to different ages, are the most abundant geological formation. In the latter Gandharan sites in Afghanistan stucco and clay artworks are frequently found, as these materials are easily available on site.
(C.R., S.P.)

[10] Di Florio et al. 1993, pp. 357-372; Faccenna et al. 1993, pp. 257-270; Olivieri 2006, pp. 137-156.

[11] See Olivieri, in this issue.

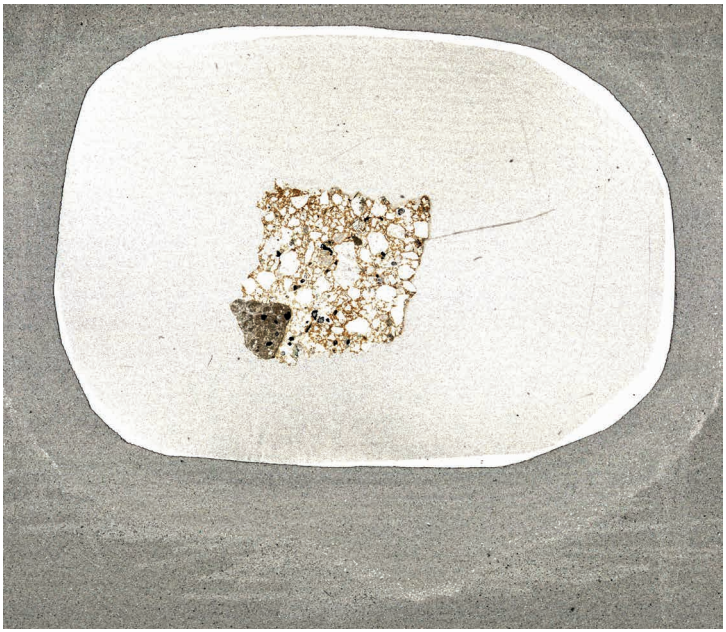

Fig. 40
Sample 1 of clay artefact from Tapa Sardar, Afghanistan. Thin section of sample: the glass slide is 48 mm across, and the fragment is 10 mm across.

Fig. 41
Sample 1 of clay artefact from Tapa Sardar, Afghanistan. Microscopic overview of the sample. The colorless grains are quartz and feldspar. The large fragment in the lower left is a biogenic limestone. Note the reddish/brownish pigments on the grain boundaries of the sand components. These pigments, responsible for the macroscopic red color, consist of oxidized iron bearing clay particles (petrographic microscope image: left image: 1 polar; right images + polars; image is 6.8 mm across).

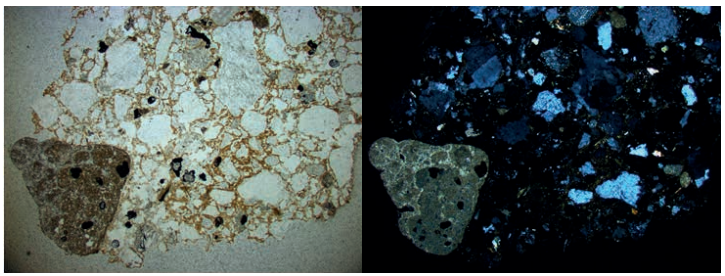

Fig. 42
Sample 1 of clay artefact from Tapa Sardar, Afghanistan. Electron Microprobe analyses.

Fig. 43
Sample 1 of clay artefact from Tapa Sardar, Afghanistan. X-ray diffraction (XRD) analysis.

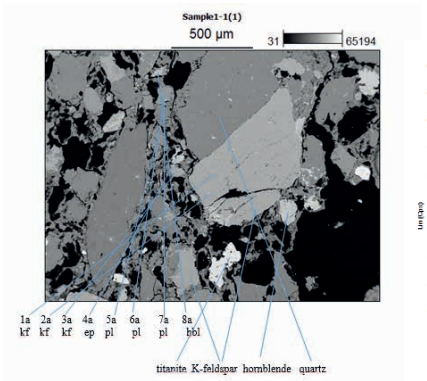

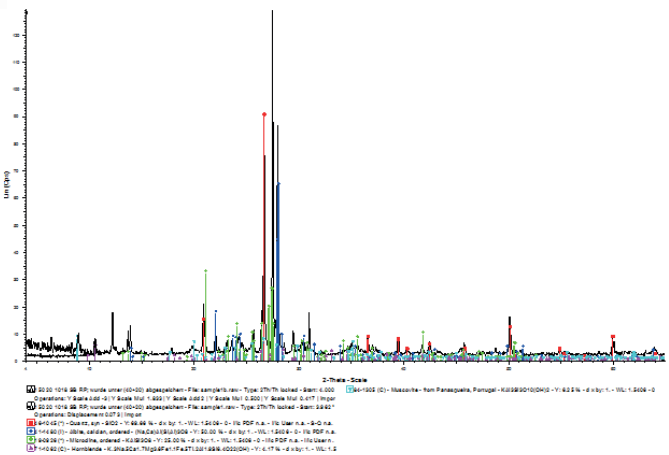

Fig. 44
Sample 2 of clay artefact from Tepe Narenj, Afghanistan. This sample is characterized by a sand fraction in which the grains are poorly attached to each other. Loose sand just from normal handling (photo T. Theye).

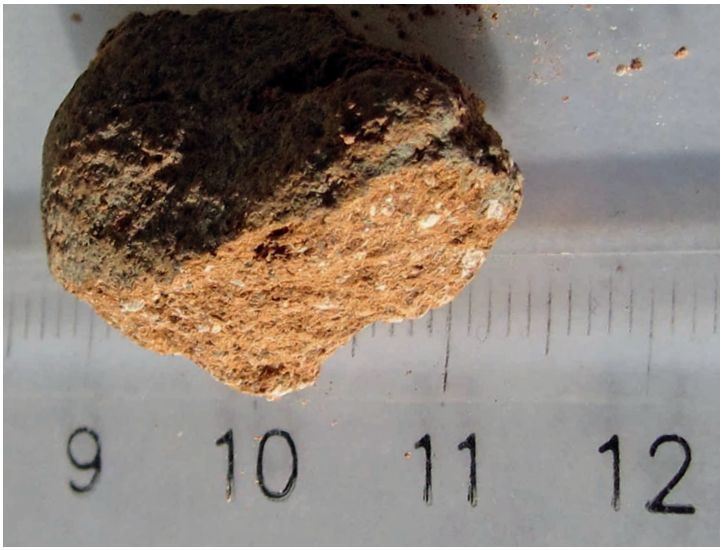

Fig. 45
Sample 2 of clay artefact from Tepe Narenj, Afghanistan: thin section of sample. The width of the image is 48 mm. A brownish component forms the majority of the brick. Note the presence of sand grains embedded in a fine-grained reddish matrix. Small grains of white matter is also present consisting of gypsum, as verified by Raman spectroscopy and electron microprobe.

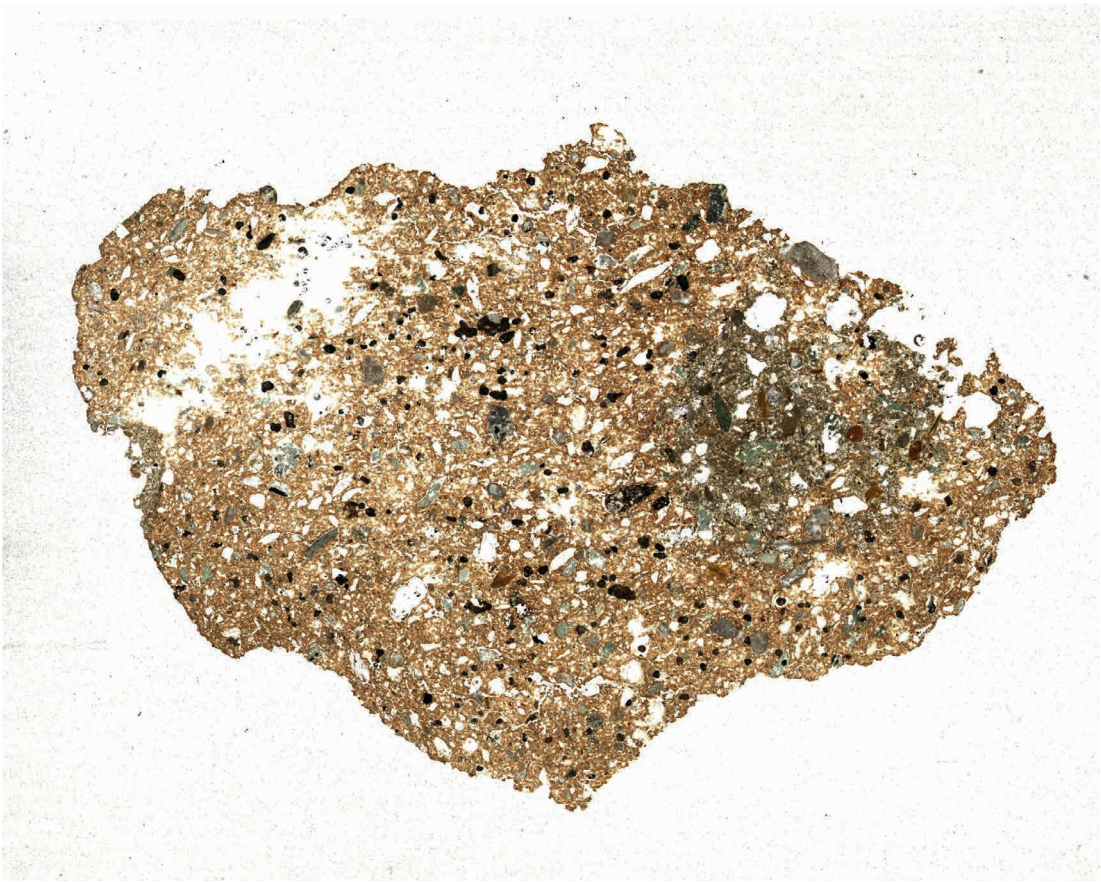

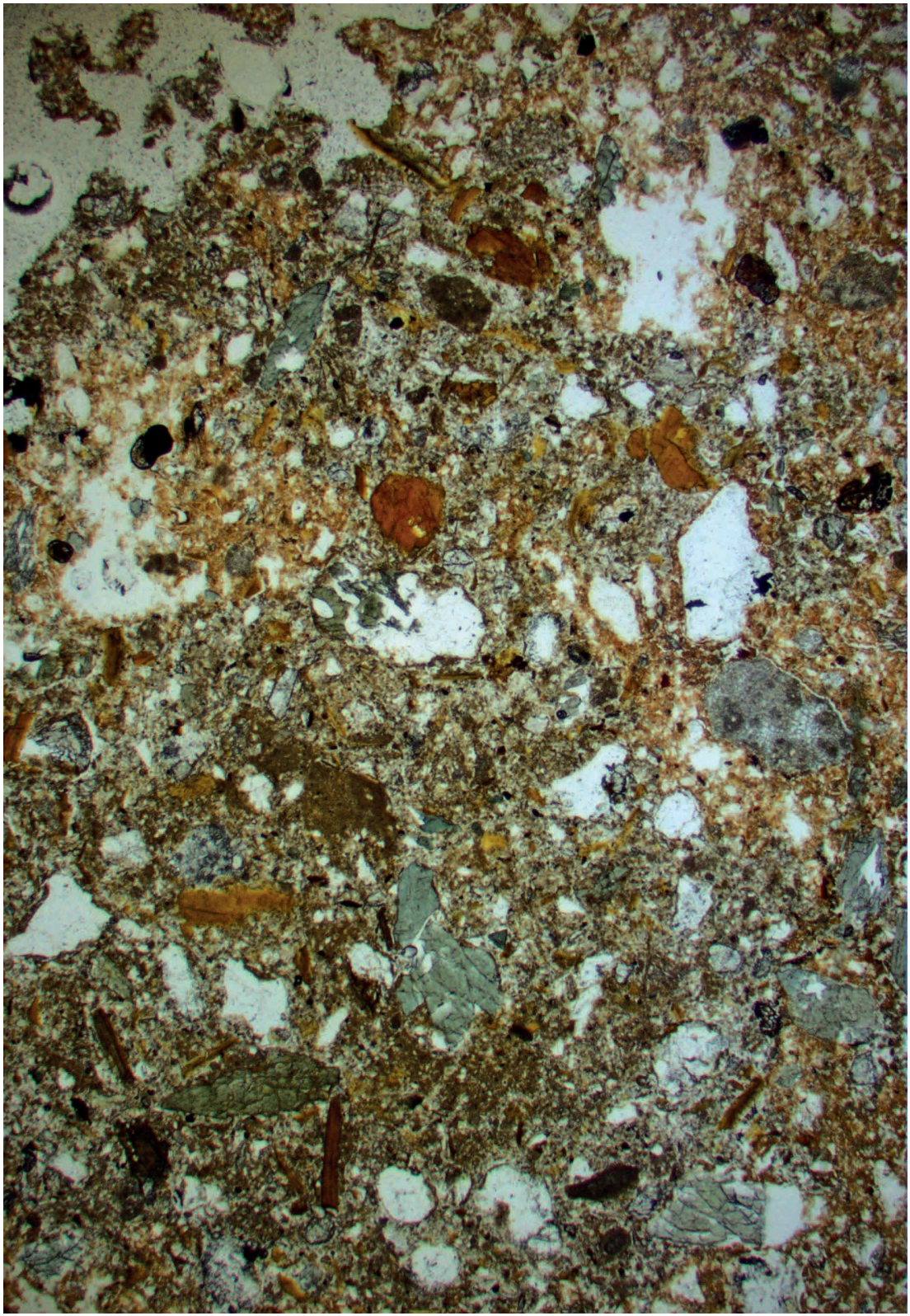

Fig. 47 a, b
Sample 2 of clay artefact from Tepe Narenj, Afghanistan: back-scattered electron image, detail of the microstructure of sample. Pores appear in black. The chemical composition of the binding clay fraction is shown in spectrum no. AAA(3) that shows higher concentrations of the elements O, Si, Al, Mg, Fe, Ca, and K typical for clay minerals. Chlorine is a component of the resin.

References

Arif M., Moon C. J. 2007, *Nickel-rich chromian muscovite from the Indus suture ophiolite, NW Pakistan: Implications for emerald genesis and exploration*, «Geochemical Journal», 41, pp.475-482.

Di Florio M. R. et al. 1993, *Lithological Analysis of Materials used in the Buildings of the Sacred Area of Pānṛ I (Swāt Valley, Northern Pakistan) and their Origins*, in D. Faccenna, A.K Khan, I.H. Nadiem, *Pānṛ I (Swāt, Pakistan)*, IsMEO Reports and Memoirs, XXVI. 1, Rome, pp. 357-372.

Ding L., Kapp P., Wan X. 2005, *Paleocene–Eocene record of ophiolite obduction and initial India-Asia collision, south central Tibet*, «Tectonics», 24,pp.1-18, [online] TC3001, doi:10.1029/2004TC001729

Dipietro J. A., Lawrence R. D. 1991, *Himalayan structure and metamorphism south of the Main Mantle Thrust, lower Swat, Pakistan*, «Journal of Metamorphic Geology », pp. 481-495.

Faccenna C. et al. 1993, *Geo-Archaeology of the Swāt Valley (NWFP, Pakistan) in the Chārbāgh-Barikoṭ Stretch. Preliminary Note*, «East and West», 43, 1-4, pp. 257-270.

Olivieri L. M. 2006, *Per Saxa. Il contributo della Missione Italiana allo studio geo-archeologico e dei manufatti rupestri nello Swat*, in Callieri P. (ed.), *Architetti, capomastri, artigiani. L'organizzazione dei cantieri e della produzione artistica nell'Asia ellenistica,* (Serie Orientale Roma), Roma, pp. 137-156.

Olivieri L.M. 2019, *A short note on contexts and chronology of the materials from Saidu Sharif, Amluk-dara, Gumbat and Barikot (Swat)*, «Restauro Archeologico», in this issue.

Gansser A. 1980, *The significance of the Himalayan suture zone*, «Tectonophysics», 62, pp.31-52.

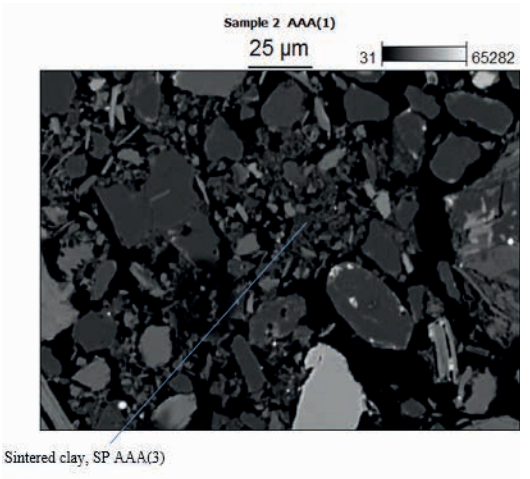

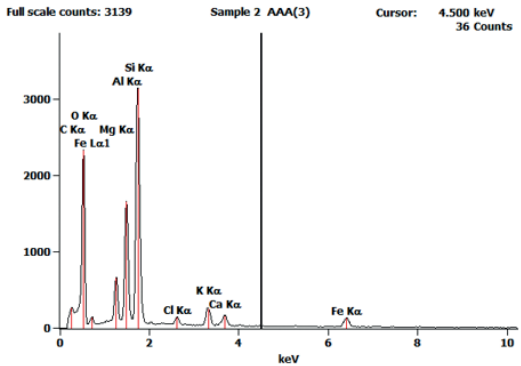

Live Time: 6.6 sec.

Acc.Voltage: 15.0 kV Take Off Angle: 40.0 deg.
Quantitative Results for: Sample 2, AAA(1)

Element	Weight %	Atom %	Atom % Error	Compnd %
O	45.55S	61.66	+/- 0.70	---
Mg	4.03	3.59	+/- 0.10	6.69
Al	10.75	8.61	+/- 0.14	20.27
Si	24.90	19.20	+/- 0.16	53.27
Cl	1.16	0.71	+/- 0.03	1.16
K	3.56	1.97	+/- 0.05	4.29
Ca	2.30	1.24	+/- 0.04	3.22
Fe	7.76	3.01	+/- 0.18	11.10
Total	100.00	100.00		100.00

Kazmi A. H. et al. 1984, *Geology of the Indus suture zone in the Mingora-Shangla area of Swat, N. Pakistan*, «Geological Bulletin» (University of Peshawar), pp.7, 127-144.

Kazmi A. H. et al. 1986, *Mingora emerald deposits (Pakistan): suture associated mineralization*, «Economic Geology», 81, pp. 2022–2028.

Jan M. Q., Tahirkheli R.A.K. 1969, *The Geology of the Lower part of Indus Kohistan (Swat), West Pakistan*, «Geological Bulletin, University of Peshawar », 4, pp.1-13.

Tahirkheli R. A. K 1979a, *Geology of Kohistan and adjoining Eurasian and Indo-Pakistan continents, Pakistan*, «Geological Bulletin, University of Peshawar. Special Issue », 11, pp. 1–30.

Tahirkheli R. A. K. 1979b, *Geotectonic Evolution of Kohistan*, «Geological Bulletin, University of Peshawar. Special Issue », 11, pp.113-130.

Tahirkheli R. A. K. 1980, *Major tectonic Scars of Peshawar Vale and Adjoining Areas, and Associated Magmatism*, «Geological Bulletin, University of Peshawar. Special Issue » 13, pp.39-46.

Tahirkheli R. A. K. et al. 1979, *The India-Eurasia suture zone in northern Pakistan; synthesis and interpretation of recent data at plate scale*, in Farah A., De Jong K.(eds), *Geodynamics of Pakistan*, Quetta, pp. 125-130.

Yin A., Mark Harrison T.M. 2000, *Geologic Evolution of the Himalayan Tibetan Orogen*, «Annu. Rev. Earth Planet. Sci.», 28, pp.211–80.

Williams V. S., Pasha M. K., Sheikh I. M. 1988-90, *Geologic Map of the Islamabad-Rawalpindi Area, Punjab, Northern Pakistan*, in U.S. Geological Survey, Department Of The Interior, Open-File Report 99-47, Quetta-Islamabad, pp.1-16.

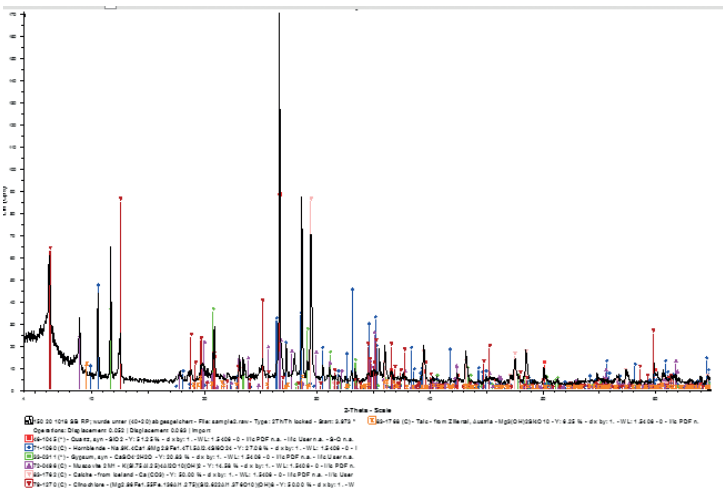

Fig. 48
Sample 2 of clay artefact from Tepe Narenj, Afghanistan: X-ray diffractogram of sample. The following phases can be recognized: quartz, plagioclase (albite), K-feldspar, hornblende, muscovite, calcite, and gypsum.